

A Holographic-moiré Technique to Obtain Separate Patterns for Components of Displacement

A combination of dual-beam holographic interferometry and moiré, provide a practical solution to the problem of the optical separation of displacement components. Results show that the technique makes holographic interferometry very useful for stress analysis

by C. A. Sciammarella and J. A. Gilbert

ABSTRACT—A symmetrical double-beam illumination is used in conjunction with a fictitious fringe system to obtain a moiré pattern which represents the projection of the displacement vector into a single plane. The fictitious system of fringes is generated by a rotation of the photographic plate. This additional degree of freedom makes it possible to optically superimpose holograms, to apply spatial filtering techniques, and to control fringe localization. The method is applicable for displacement determination throughout the entire holographic range. A disk subjected to diametral compression is used to demonstrate that displacements and strains on the order of magnitude of those found in real engineering problems can be determined very accurately.

List of Symbols

- \underline{d} = displacement vector
- \underline{d}_x = scalar component of the displacement
- $f(u)$ = function of the fictitious displacement
- \underline{g} = sensitivity vector
- $\underline{i}, \underline{j}, \underline{k}$ = basis of unit vectors
- $\underline{k}_1, \underline{k}_1', \underline{k}_2, \underline{k}_2'$ = propagation vectors
- $\underline{n}_1, \underline{n}_2, \underline{n}_R$ = normal vectors
- n_1, n_2, n_R = fringe-order numbers
- u, v = scalar components of the displacement
- x, y, z = coordinates of reference system
- z_c = z coordinate of the center of rotation
- C = rotation axis
- D = distance from the localization surface to the hologram; diameter of the disk
- D' = distance between the object and the holographic plate
- \underline{H} = rotation vector
- P = point on object surface
- P' = point on localization surface
- P_1, P_1', P_2 = points on the photographic plate
- \underline{R} = position vector from the center of rotation to a point on the photographic plate
- α = angle between the illumination beams and the normal to the object surface

β, β_x, β_y = angles of rotation of the photographic plate

δ, δ' = phase changes

δ_1, δ_m = fringe spacing

ϵ_x, ϵ_y = components of strain

θ = angle between observation or illumination directions and the normal to the object surface

θ_P = angle between a scattered ray and the normal to the photographic plate

θ_R = angle between the reference beam and the normal to the photographic plate

$\Delta\theta_P, \Delta\theta_P', \Delta\theta_R$ = changes in angle

λ = wavelength of the laser light

$\phi, \phi_1, \phi_2, \phi_R$ = phase relations

Introduction

A fundamental property of holographic interferometry, when applied to diffusing surfaces, is to provide displacement information along a sensitivity vector.

In Fig. 1, a point P moves through a displacement

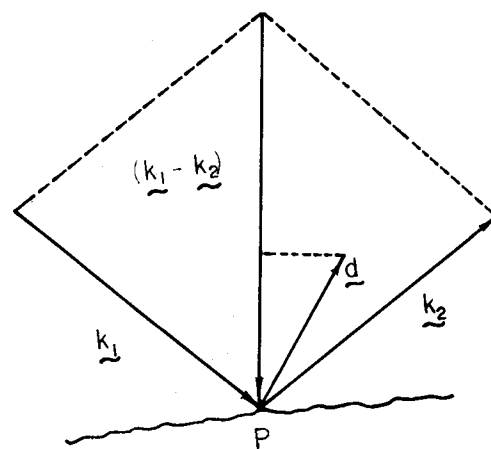


Fig. 1—Determination of the displacement at a point by means of holographic interferometry

C. A. Sciammarella is Professor of Mechanics and Mechanical Engineering, Illinois Institute of Technology, Chicago, IL 60616. J. Gilbert is Assistant Professor, University of Wisconsin at Milwaukee, Milwaukee, WI.

Paper was presented at 1975 SESA Spring Meeting held in Chicago, IL on May 11-16.

given by the vector \underline{d} . The illumination direction is characterized by the propagation vector \underline{k}_1 ; the observation direction by \underline{k}_2 . The resulting holographic-fringe pattern is indicative of a phase change, δ , which gives information about one projected component of the displacement. That is,

$$\delta = (\underline{k}_1 - \underline{k}_2) \cdot \underline{d} = \underline{g} \cdot \underline{d} \quad (1)$$

where \underline{g} is the sensitivity vector.

In a limited number of problems, it is possible to use a single object beam to obtain holographic

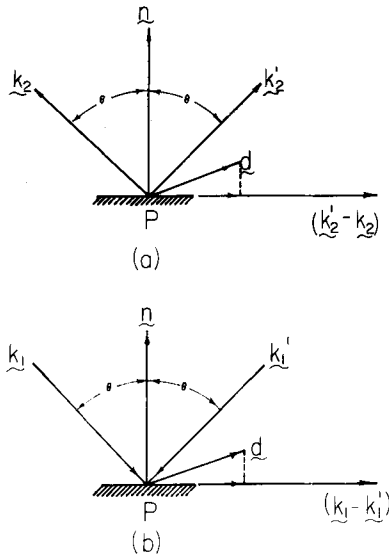


Fig. 2—Holographic determination of in-plane displacement. (a) Double observation; (b) double illumination

patterns which correspond to only one component of the displacement throughout the entire field of observation.^{1,2}

Ennos describes a technique to obtain the in-plane component of the displacement vector of a point.³ The method consists of making simultaneous exposures of two holographic plates before and after an object is loaded. If a point on the object is viewed obliquely through these two holograms at equal angles to the surface normal as shown in Fig. 2(a), one can write

$$\delta = (\underline{k}_1 - \underline{k}_2) \cdot \underline{d} \quad (2)$$

and

$$\delta' = (\underline{k}_1 - \underline{k}_2') \cdot \underline{d} \quad (3)$$

Subtracting eq (3) from eq (2) one obtains

$$\delta - \delta' = (\underline{k}_2' - \underline{k}_2) \cdot \underline{d} \quad (4)$$

where $(\underline{k}_2' - \underline{k}_2)$ is a vector lying on the surface of the object. Ennos suggests a solution of eq (4) by computing the difference of the orders in the two patterns.

Utilizing the fact that the point of observation can be interchanged with the point of illumination, Butters⁴ and Boone⁵ replaced the double observation by a dual illumination. In this case, Fig. 2(b), eq (4) becomes

$$\delta - \delta' = (\underline{k}_1 - \underline{k}_1') \cdot \underline{d} \quad (5)$$

The sensitivity vector becomes independent of the direction of observation.

In both cases, the information can be retrieved by superimposing the two obtained patterns and observing the resulting moiré pattern.⁶

The practical realization of this idea has been hindered by the difficulty in obtaining systems of fringes capable of generating good-quality moiré patterns.

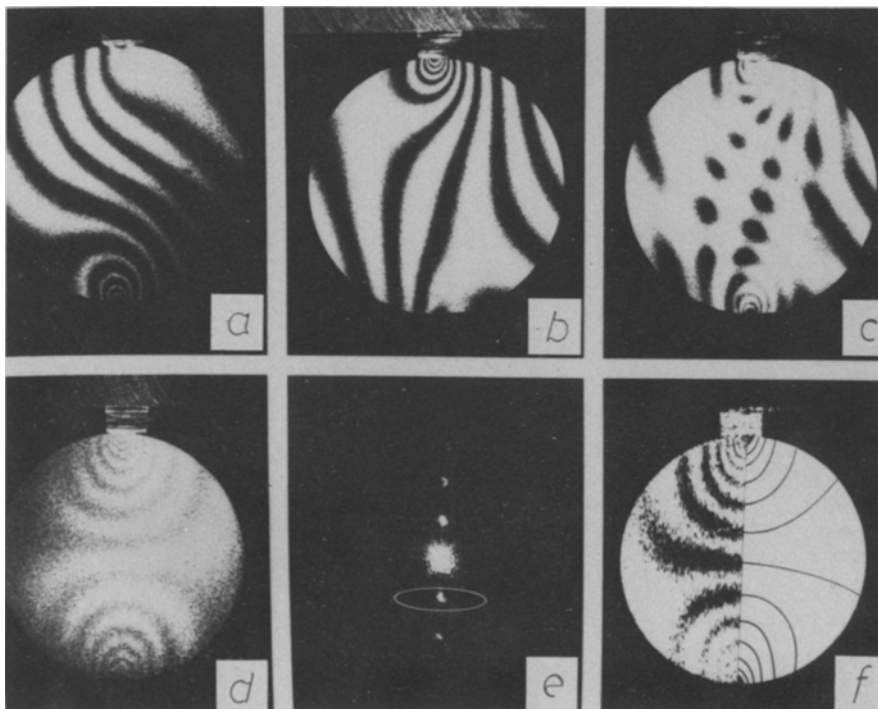


Fig. 3—In-plane displacement with dual illumination. (a), (b) Single-beam patterns; (c) superposition of (a) and (b); (d) same as (c) but with an initial pattern; (e), (f) diffraction pattern of (d) and filtered image

Basic Theory of the Phase Subtraction by Means of the Moiré Method

The dual-illumination approach is used throughout this paper. This method has a distinct advantage over the double-observation method. That is, with this technique it is possible to optically superimpose the component patterns before reconstruction.

Localization problems or fringe characteristics, such as spacing, gradient and orientation, often make the optical subtraction or moiré of the component patterns difficult or impossible to observe. The ideal solution to the problem of optically subtracting the two patterns is to have an initial pattern with high fringe density. If a dual illumination is used, this initial pattern must satisfy the following prerequisites:

(a) The fringe loci and pitch of the initial pattern must be the same for both illuminating beams, (b) the plane of localization of the pattern must be coincident with the surface of the model, (c) the initial pattern must be produced by simple means, which do not require the displacement of the model.

If the above conditions are satisfied, the phase of the initial pattern is given by the equation

$$\phi(f(u)) = n\lambda \quad (6)$$

where $f(u)$ is a function of the fictitious initial displacement.

When the model is loaded, each illumination adds a different contribution to the initial phase and two patterns result which are characterized by

$$\phi_1 [f(u) + \underbrace{(k_1 - k_2)}_{\sim} \cdot \underbrace{d}_{\sim}] = n_1 \lambda \quad (7)$$

and

$$\phi_2 [f(u) + \underbrace{(k_1' - k_2)}_{\sim} \cdot \underbrace{d}_{\sim}] = n_2 \lambda \quad (8)$$

The moiré pattern produced by the two patterns is given by the equation

$$\phi_1 [f(u) + \underbrace{(k_1 - k_2)}_{\sim} \cdot \underbrace{d}_{\sim}] - \phi_2 [f(u) + \underbrace{(k_1' - k_2)}_{\sim} \cdot \underbrace{d}_{\sim}] = (n_1 - n_2) \lambda \quad (9)$$

or

$$\phi_R [\underbrace{(k_1 - k_1')}_{\sim} \cdot \underbrace{d}_{\sim}] = n_R \lambda \quad (10)$$

The moiré pattern displays the in-plane component of the displacement vector; however, there is an important difference between the latter and a moiré pattern produced by a line grating printed on the surface of the model. The moiré method is insensitive to translations parallel to the plane of the grating. It can be easily checked that this is not the case for the moiré pattern generated by the two families of holographic fringes. A translation generates two systems of parallel fringes with different pitch, capable of producing a moiré pattern.

The need for the introduction of a fictitious displacement, common to each component pattern, is evident in Fig. 3. A disk under diametral compression was illuminated in order to isolate the displacement parallel to the direction of loading. Figures 3(a) and 3(b) show the holograms corresponding to each illumination beam.

Figure 3(c) shows the simultaneous reconstruction of both holograms. Although the moiré pattern is inherent in this combination, it could not be observed directly or extracted by optical-filtering techniques.

On the other hand, Fig. 3(d) shows the case where

an initial pattern has been added to each of the component patterns. The moiré is readily observed and optical-filtering techniques can be applied. Figure 3(e) shows the diffraction pattern produced by the two interfering systems of fringes and the order utilized to filter the resulting moiré pattern. Figure 3(f) shows the moiré pattern after filtering.

The observed pattern is independent of the orientation of the initial system of fringes. Figure 4 shows two half patterns generated with orthogonal systems of initial fringes. The two patterns match perfectly.

Generation of the Initial Patterns

The successful implementation of the described technique requires the generation of initial patterns satisfying the prerequisites previously indicated. There are many methods which can be used to gen-

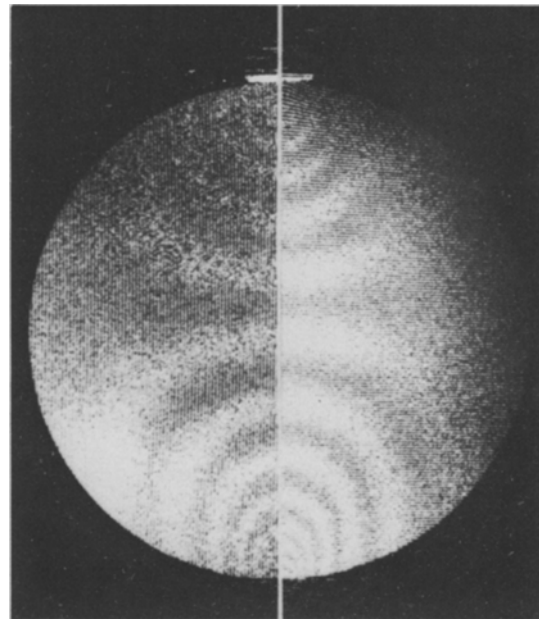


Fig. 4—The displacement component parallel to the direction of loading of a disk subjected to diametral compression—Left and right halves are generated with vertical and horizontal initial patterns

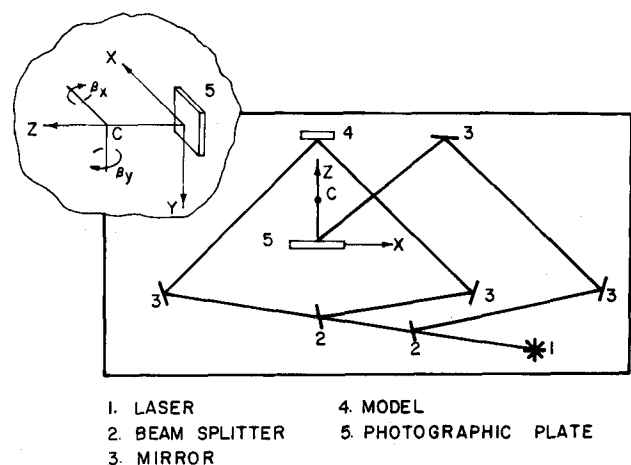


Fig. 5—Experimental setup and coordinate system

erate initial patterns. One simple way is to displace the holographic plate between exposures. This is the solution that has been adopted in the present paper.

Figure 5 shows the basic setup used to register the holograms. Two collimated beams illuminate a model which is observed from a point located along the normal to the object surface. An initial exposure of the unloaded model is made with both illuminating beams. The fictitious displacement is then introduced by rotating the holographic plate through a small angle around an axis parallel to the plane of the plate. The load is applied and a second exposure is taken.

In order to derive expressions for the fringe localization and the fringe pitch of the initial pattern, let us consider that the only hologram registered is the one corresponding to the fictitious motion.

To compute these quantities, the equations derived in Ref. 7 will be applied.

Figure 6 shows the system of coordinates used in this derivation. AB represents the surface of the object. HH is the initial position of the holographic plate and H'H' is its final position. Point C is the center of rotation. Consider an orthogonal base of unit vectors \underline{i} , \underline{j} , \underline{k} , associated with the x, y, z axis, respectively. Assume that the plate is rotated so that

$$\underline{H} = -\beta \underline{j} \quad (11)$$

The displacement vector for a point on the holographic plate is

$$\underline{d} = \underline{H} \times \underline{R} \quad (12)$$

where \underline{R} is the vector from the rotation center to the point P_1 .

The illuminating beam impinges on point P of the object. Since the surface of the model is a diffusing surface, beams emerge from P in all directions. Let us single out a particular ray which subtends an angle θ_P with respect to the normal \underline{n} of the plate. This ray interferes with a reference beam which makes an angle θ_R with the plate normal. Referring to eq (3) of Ref. 7, this interference generates fringes with spatial frequency characterized by the fringe spacing

$$\delta_1 = \frac{\lambda}{\sin \theta_R - \sin \theta_P} \quad (13)$$

When the plate is rotated and a second exposure is taken, the specified ray generates a slightly different fringe spacing at point P_2 . Let us assume that the hologram is developed, placed back in its rotated position and reconstructed. The beam emanating from point P_2 goes back to P. The point P_1 has moved to P_1' and the beam corresponding to the initial beam PP_1 , experiences a change of direction $\Delta\theta_P$. The point of intersection of the two beams at P' defines the region of maximum contrast of the interference fringes produced by holographic interferometry.⁷ This is the localization surface. Beams P_2P' and $P_1'P'$ are referred to as homologous rays.⁸ To obtain the position of P' , we need to compute the change of direction $\Delta\theta_P$.

In order to establish the change in θ_P when the plate is rotated through an angle β , it is necessary to differentiate eq (13). That is

$$\Delta\theta_R \cos \theta_R - \Delta\theta_P' \cos \theta_P = 0 \quad (14)$$

where $\Delta\theta_P'$ is the change in angle with respect to $\underline{n}_{P'}$. Now

$$\Delta\theta_R = -\beta \quad (15)$$

Substituting the above into eq (14),

$$\Delta\theta_P' = -\beta \frac{\cos \theta_R}{\cos \theta_P} \quad (16)$$

The change in θ_P referred to the original position of the plate is

$$\Delta\theta_P = \beta + \Delta\theta_P' \quad (17)$$

Using eq (16), the above becomes

$$\Delta\theta_P = \frac{\beta}{\cos \theta_P} (\cos \theta_P - \cos \theta_R) \quad (18)$$

If D is the distance from the localization surface to the hologram, we can write

$$\Delta\theta_P = \frac{|\underline{d}|}{D} \cos \theta_P \quad (19)$$

where $|\underline{d}|$ is the magnitude of the displacement vector. Using eqs (11) and (12)

$$\Delta\theta_P = \frac{\beta \sqrt{x^2 + z_c^2}}{D} \cos \theta_P \quad (20)$$

where z_c is the coordinate of the center of rotation. The above equation can be written

$$\Delta\theta_P = \frac{\beta z_c \sqrt{1 + \left(\frac{x}{z_c}\right)^2}}{D} \cos \theta_P \quad (21)$$

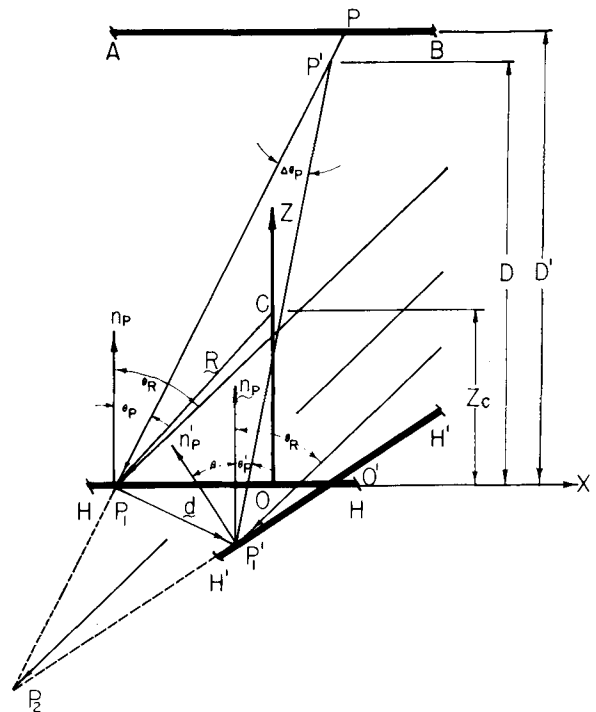


Fig. 6—Localization of holographic fringes for a rotation of the photographic plate

From eqs (18) and (21), we obtain

Introducing eq (24) in eq (22), one obtains

$$D = \frac{z_c \sqrt{1 + \left(\frac{x}{z_c}\right)^2}}{\left[1 + \left(\frac{x - x_P}{D}\right)^2\right] \left[\frac{1}{\sqrt{1 + \left(\frac{x - x_P}{D}\right)^2}} - \cos \theta_R\right]} \quad (25)$$

$$D = \frac{z_c \cos^2 \theta_P \sqrt{1 + \left(\frac{x}{z_c}\right)^2}}{\cos \theta_P - \cos \theta_R} \quad (22)$$

If D' is the distance between the object and the holographic plate

$$\cos \theta_P = \frac{D'}{\sqrt{(x - x_P)^2 + (D')^2}} \quad (23)$$

If the localization is on the object surface, $D = D'$. Hence

$$\cos \theta_P = \frac{1}{\sqrt{1 + \left(\frac{x - x_P}{D}\right)^2}} \quad (24)$$

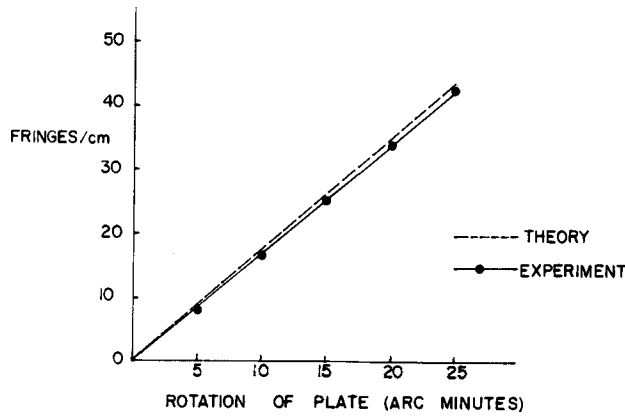


Fig. 7—Theoretical and experimental values of the fringe spacing produced by a rotation of the photographic plate

If one assumes that the distance D is large as compared to the lateral dimensions of the model, that the direction of observation is predominantly in the direction of the normal to the object, and that during the reconstruction the entrance pupil of the reconstructing lens limits the aperture of the beam to a small angle, then the quantity $\frac{x - x_P}{D}$ can be neglected in eq (25). Furthermore, if $\left(\frac{x}{z_c}\right)^2$ can be neglected with respect to 1, eq (25) reduces to

$$D = \frac{z_c}{1 - \cos \theta_R} \quad (26)$$

With the restriction emanating from the assumptions used in the derivation, the localization plane depends only on the coordinate of the rotation center and on the angle of illumination of the reference beam.

The fringe spacing can be computed by means of eq (16) of Ref. 7, that is,

$$\delta_m = \frac{\lambda}{\Delta \theta_P \cos \theta_P} \quad (27)$$

Using eq (21) and neglecting the quantity $\left(\frac{x}{z_c}\right)^2$ with respect to one, we obtain

$$\delta_m = \frac{\lambda D}{\beta z_c} \quad (28)$$

Equation (26) has been experimentally checked and an excellent agreement has been obtained between observed and computed values.

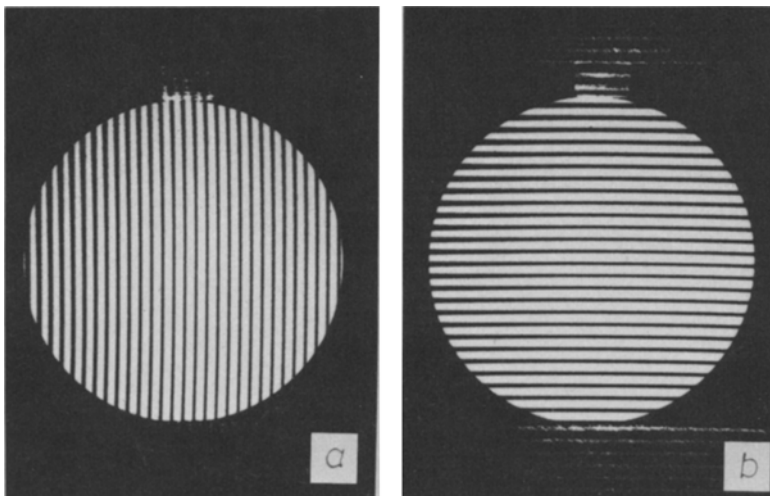


Fig. 8—Initial patterns for orthogonal rotations of photographic plate

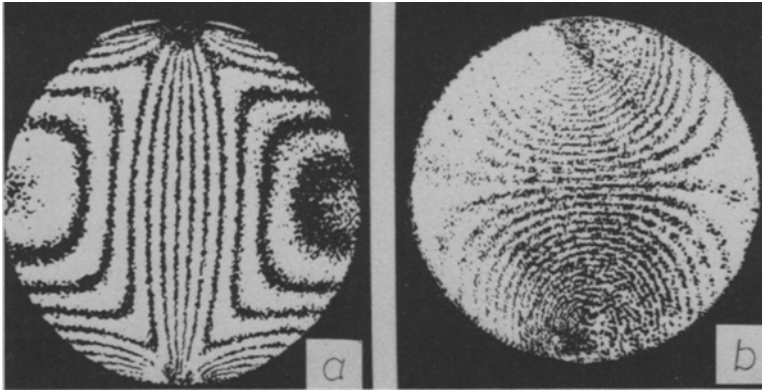


Fig. 9—In-plane displacement of a 63.5-mm-diam disk subjected to diametral compression. Each fringe corresponds to a displacement of 4.5×10^{-4} mm. (a) U pattern, (b) V pattern

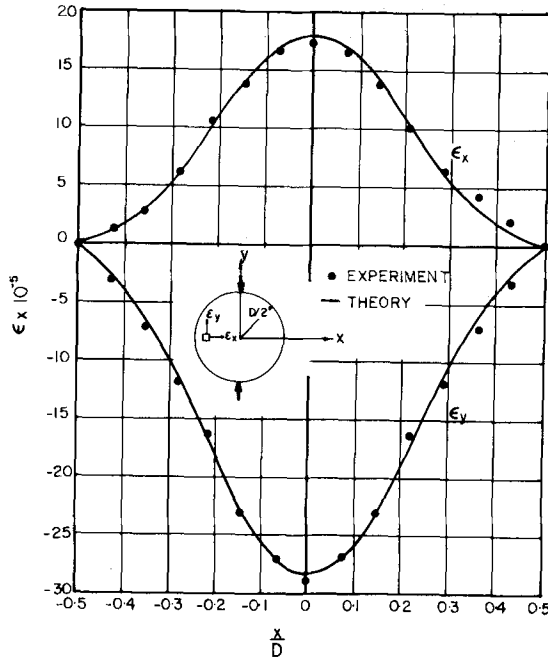


Fig. 10—Theoretical and experimental strains along the horizontal center line of a disk subjected to diametral compression

Figure 7 shows the experimentally measured fringe spacings and the values obtained by means of eq (28). A very good agreement is observed between experimental and theoretical values. The deviation for 25 min of arc is approximately three percent.

Experimental

Figure 5 shows the setup utilized in the experiments. The holographic plate is supported in a kinematic device. This device has controlled displacement in the direction perpendicular to the plate which makes it possible to precisely locate the point C. The plate allows rotations to be made around a vertical or a horizontal axis, Fig. 8. The angle α , between the normal to the object surface and each illuminating beam controls the sensitivity that can be ob-

tained with the system. From eq (5) one can obtain

$$d_x = \frac{n \lambda}{2 \sin \alpha} \quad (29)$$

where d_x is the component of the displacement in the x-direction. Provided that the diffusing properties of the surface are such that enough intensity is obtained to expose the holographic plate, maximum sensitivity is obtained with grazing incidence.

Figure 9 shows the u and v patterns corresponding to a disk under diametral compression. Figure 10 shows the ϵ_x and ϵ_y strains, plotted together with the theoretical values. All patterns shown correspond to illuminations at $\alpha = 45$ deg.

Conclusions

The problem of separating in-plane components of displacement in holographic interferometry by optical means has been solved. This solution is a practical one and requires only simple devices. The technology introduced in this paper is a decisive step forward in the utilization of holographic interferometry as a practical tool of stress analysis. Further work is being done to extend the techniques introduced in this paper to 3-D surfaces. The question of optically obtaining patterns for the derivatives of the displacement is also under investigation. This work will be reported in future papers.

References

1. Wilson, A. D., "Holographically Observed Torsion in a Cylindrical Shaft," *Ap. Opt.*, 9 (9) (1970).
2. Wilson, A. D., "In-Plane Displacement of a Stressed Membrane with a Hole Measured by Holographic Interferometry," *Ap. Opt.*, 10 (4) (1971).
3. Ennos, A. E., "Measurement of In-Plane Surface Strains by Hologram Interferometry," *J. of Phys. E., Sci. Instr.* (1) (1968).
4. Butters, J. N., "Application of Holography to Instrument Diaphragm Deformations and Associated Topics," *The Engineering Uses of Holography*, Cambridge Univ. Press, London, New York (1970).
5. Boone, P. M., "Holographic Determination of In-Plane Deformation," *Opt. Technol.*, 2 (1970).
6. Abranson, N., "The Holo-Diagram VI; Practical Device in Coherent Optics," *Ap. Opt.*, 11 (11) (1972).
7. Sciammarella, C. A., "Holographic Interferometry Analyzed from the Point of View of Moiré Patterns," *Exp. Mech. in Res. and Dev., Proc. of Int. Symp. on Exp. Mech., Univ. of Waterloo, June 12-16, 1972*.
8. Viénot, J., et al, "Hologram Interferometry: Surface Displacement Fringe Analysis as an Approach to the Study of Mechanical Strains and other Application to the Determination of Anisotropy in Transparent Objects," *The Engineering Uses of Holography*, Cambridge Univ. Press, London, New York (1970).